RESEARCH ARTICLE

Medioresinol from Eucommiae cortex improves myocardial infarction-induced heart failure through activation of the PI3K/AKT/mTOR pathway: A network analysis and experimental study

Xueting Qin[1]◎, Xuan Liu[2]◎, Can Guo[2], Li Huang[2], Qiyao Xu[1,2] *

1 Nephrology, The Second People's Hospital of China Three Gorges University, Yichang, Hubei, China,
2 Graduate School, Nanjing University of Chinese Medicine, Nanjing, Jiangsu, China

◎ These authors contributed equally to this work.
* dr_xuqiyao@njucm.edu.cn

Abstract

Objective

This study aims to systematically analyze the potential active components of Eucommiae cortex in the treatment of post- myocardial infarction heart failure through network analysis and molecular docking methods. In vitro experiments were conducted to verify that medioresinol, a component of Eucommiae cortex, improves oxygen-glucose deprivation-induced cell failure through its anti-inflammatory and antioxidant capacities.

Methods

Potential active components of Eucommiae cortex were screened using specific data. The targets of these components were predicted using Swiss Institute of Bioinformatics database and TargetNet, and key targets were identified by intersecting with the disease targets of myocardial infarction and heart failure. Protein-Protein Interaction analysis was performed on the key targets to screen for core targets. Genomics Institute of the Novartis Research Foundation and Human Protein Atlas were used to identify myocardial highly expressed targets. Kyoto Encyclopedia of Genes and Genomes and Gene Ontology enrichment analyses were conducted using the Database for Annotation, Visualization, and Integrated Discovery. Molecular docking was performed for the final components and target proteins. In vitro experiments were carried out using H9c2 cells subjected to oxygen and glucose deprivation conditions to validate the effects of the screened potential active components.

Results

Network analysis revealed that Eucommiae cortex might exert its effects through the phosphoinositide 3-kinase/protein kinase B/mammalian target of rapamycin (PI3K/AKT/mTOR),

hypoxia-inducible factor 1, and Janus kinase/signal transducer and activator of transcription pathways, which are crucial for myocardial contraction, vascular tone regulation, inflammatory response, and oxidative stress. Molecular docking indicated stable binding of the selected compounds to PI3K, AKT, and mTOR. Medioresinol was selected for further study and shown to significantly improve oxidative stress and inflammatory response in myocardial ischemia-hypoxia model cells by activating the PI3K/AKT/mTOR pathway.

Conclusion

This study confirms the role of the PI3K/AKT/mTOR pathway in the cardiovascular protective effects of Eucommiae cortex and provides evidence at the cellular level. Medioresinol demonstrated potential therapeutic effects on myocardial infarction induced heart failure by reducing oxidative stress and inflammatory responses. These findings offer a theoretical basis for the application of Eucommiae cortex in the treatment of heart failure and support the development of new therapeutic drugs for cardiovascular diseases. Future research should further validate these effects in animal models and explore the overall efficacy of Eucommiae cortex.

Introduction

Heart failure (HF) represents the terminal stage of cardiovascular diseases, characterized by a complex pathogenesis involving various factors such as myocardial injury, neuroendocrine activation, inflammatory responses, and oxidative stress [1, 2]. The primary underlying causes of HF include hypertension, diabetes, and coronary artery disease, with myocardial infarction (MI) being a significant contributor to HF among coronary artery disease patients [3, 4]. Post-MI HF (post-MI HF) has a relatively high incidence. Although the risk of HF after MI has significantly decreased with the widespread use of reperfusion therapy, approximately 10% of ST-elevation MI patients still develop HF within the following years [5, 6]. The main reasons for HF after MI include myocardial cell necrosis and fibrosis [7]. On one hand, the reduction and loss of function of local myocardium post-MI can lead to acute HF; on the other hand, short-term inflammatory responses and long-term myocardial remodeling after MI can result in chronic HF. The treatment of post-MI HF does not significantly differ from that of general HF, primarily relying on pharmacotherapy and lifestyle modifications. Commonly used medications include beta-blockers, angiotensin receptor-neprilysin inhibitors, angiotensin-converting enzyme inhibitors, angiotensin II receptor blockers, and aldosterone receptor antagonists, which can inhibit myocardial remodeling, improve cardiac function, and enhance prognosis through various mechanisms [8]. Despite significant advancements in the treatment of acute MI, post-MI HF remains difficult to fully treat, with poor prognosis. Even though many current medications benefit HF patients, the all-cause mortality rate has not further declined [9]. Therefore, there is an urgent need to explore new therapeutic strategies to improve the long-term prognosis of patients with post-MI HF or to further prevent the occurrence of HF after MI.

Traditional Chinese medicine has unique advantages in treating cardiovascular diseases due to its multi-component, multi-target, and multi-pathway therapeutic effects [10]. Eucommiae cortex, a traditional Chinese botanical drug, contains major chemical constituents such as flavonoids, lignans, and phenolic acids, which possess a wide range of pharmacological

activities [11, 12]. In traditional Chinese medicine, Eucommiae cortex is known for its properties of tonifying the liver and kidneys, strengthening bones and muscles, and preventing miscarriage. It is commonly used in the cardiovascular field to treat hypertension. Its antihypertensive effects were confirmed approximately half a century ago and are primarily attributed to its active component, pinoresinol diglucoside [13]. Modern pharmacological research has demonstrated that Eucommiae cortex also exhibits anti-inflammatory, antioxidant, anti-fibrotic, and immunomodulatory effects [14–17]. Since oxidative stress, inflammatory responses, and myocardial fibrosis are the main causes of HF following MI, Eucommiae cortex may have potential therapeutic value in the treatment of post-MI HF.

Although the pharmacological effects of Eucommiae cortex have been widely studied, its specific mechanisms in the treatment of HF remain unclear and under-researched, with studies focusing on post-MI HF being nonexistent. However, recent research suggests that the component of Eucommiae cortex, Aucubin, can effectively treat pressure overload-induced HF, primarily by activating the β(3)-adrenergic receptor/adenylyl cyclase/cyclic adenosine monophosphate pathway [18]. Due to the multi-component nature of traditional Chinese medicine, its mechanisms of action are relatively complex. To fully understand the therapeutic potential of Eucommiae cortex, it is necessary to adopt systematic research approaches to elucidate its mechanisms of action.

This study aims to systematically analyze the potential active components of Eucommiae cortex in the treatment of post-MI HF, as well as their potential targets and mechanisms, using network analysis and molecular docking methods. Furthermore, in vitro experiments will be conducted to verify the anti-inflammatory and antioxidant capacities of the screened potential active components in the treatment of MI-induced HF. It is hoped that this research will provide a theoretical basis for the application of Eucommiae cortex in the treatment of HF and offer scientific support for the development of new therapeutic drugs for HF. By systematically analyzing the multi-target and multi-pathway mechanisms of Eucommiae cortex, this study will help elucidate the holistic pharmacological action patterns of traditional Chinese medicine formulas, providing a reference for the modernization and internationalization of traditional Chinese medicine.

Materials and methods

Screening of effective components from Eucommiae cortex

Using the Traditional Chinese Medicine Systems Pharmacology Database and Analysis Platform (TCMSP, https://tcmsp.91medicine.cn/#/home), search for Eucommiae cortex, select "*ingredients*", and download the entire dataset. Filter effective components based on oral bioavailability (OB) $\geq$ 30% [19], drug-likeness (DL) $\geq$ 0.18 [20], and molecular weight (MW) < 500 [21].

Prediction of target proteins for effective components

The selected effective components were searched in PubChem to obtain their Simplified Molecular Input Line Entry System (SMILES). For those components without available SMILES, the molecular structure files (.mol2) provided by TCMSP were converted to SMILES using the Open Babel open-source tool (version 3.1.0, http://openbabel.org/). Subsequently, the potential targets were predicted using the Swiss Institute of Bioinformatics (SWISS) online tool (http://www.swisstargetprediction.ch/), selecting *Homo sapiens* and using the obtained SMILES. For molecules without predicted targets from the SWISS online tool, TargetNet (http://targetnet.scbdd.com/calcnet/index/) was used to predict the targets, with the settings

kept at default parameters (Include models with AUC ≥0.7, Fingerprint type: ECFP4 finger-prints). The obtained data retained the target's Uniprot ID and Probability information.

Acquisition of disease targets

The targets for diseases were obtained using the DisGeNET database (https://www.disgenet.org/search). Specifically, searches were conducted for heart failure (CUI: C0018801) and myocardial infarction (CUI: C0027051). By clicking on "Summary of Gene-Disease Associations," the resulting data were saved, retaining the information on *Gene*, *Full name*, and *Uniprot ID*.

PPI and key targets

The targets obtained in sections "prediction of target proteins for effective components" and "acquisition of disease targets" were intersected based on their Uniprot IDs to identify shared targets. The shared targets were then uploaded in bulk to the String database (https://string-db.org/) using the "Multiple proteins" function in the Search section, with the organism set to Homo sapiens. The resulting protein-protein interaction (PPI) data were directly imported into Cytoscape (version 3.10.2, https://cytoscape.org/). Using the Molecular Complex Detection plugin (degree cutoff: 2, k-core: 2), clusters with a node count of 4 or more were selected as core clusters. Subsequently, the Cytohubba plugin was used to further screen the targets in the core clusters, selecting the top 15 targets based on the Degree score and the top 15 targets based on the maximal clique centrality (MCC) score. The intersection of these two target groups was then taken to identify the key targets.

KEGG pathway enrichment analysis and GO functional enrichment analysis

The targets obtained in sections "prediction of target proteins for effective components" and "acquisition of disease targets" were intersected based on their Uniprot IDs to identify shared targets. The Uniprot IDs of these shared targets were then uploaded in bulk to the Database for Annotation, Visualization, and Integrated Discovery (DAVID) (https://david.ncifcrf.gov/tools.jsp) for analysis. Data were extracted for the following four categories: Kyoto Encyclopedia of Genes and Genomes (KEGG) Pathway and Gene Ontology biological process (GOBP) terms Direct, GO cellular component (GOCC) terms Direct, and GO molecular function (GOMF) terms Direct. The results were saved as separate Excel files. For each table, entries with p-values, Bonferroni values, Benjamini values, and FDR values all less than 0.05 were selected. If the final data count exceeded 20, the 20 entries with the smallest p-values were retained. The data were then visualized in Python (version 3.11.7, https://www.python.org/) using pandas (version 2.2.2, https://pandas.pydata.org/), matplotlib (version 3.8.0, https://matplotlib.org/), and numpy (version 1.26.4,).

Screening for highly expressed myocardial target proteins

Using the same method as described in section "KEGG pathway enrichment analysis and GO functional enrichment analysis", the shared targets were imported into the DAVID database to extract Genomics Institute of the Novartis Research Foundation and Human Protein Atlas data. The proteins expressed in myocardial tissue were then filtered and selected.

Screening for highly enriched KEGG and GO in myocardium

The target proteins obtained in section "screening for highly expressed myocardial target proteins" were merged based on their Uniprot IDs. The final list of highly expressed myocardial

proteins was then imported into the DAVID database to extract and visualize KEGG and GO data using the method described in section "KEGG pathway enrichment analysis and GO functional enrichment analysis".

Construction of compound-target-KEGG/GO-disease network

The key proteins obtained in section "screening for highly expressed myocardial target proteins", the key KEGG and GO terms screened in section "screening for highly enriched KEGG and GO in myocardium", and the effective components of Eucommia targeting these key proteins were matched with the diseases to construct the compound-target-KEGG/GO-disease network. The network was visualized using Gephi software (version 0.10.1, https://gephi.org/).

Molecular docking

Molecular docking was performed for the proteins and effective components of Eucommia mentioned in section "construction of compound-target-KEGG/GO-disease network". The 3D structure files of the effective components were obtained from PubChem. If 3D structure files were not available, 2D structure files provided by TCMSP were converted to 3D structure files using Open Babel. Target proteins were searched on the Uniprot website using their Uniprot IDs. The structural data were reviewed to select the highest resolution single-chain structures, and the corresponding structure files were obtained from the RCSB Protein Data Bank (https://www.rcsb.org/).

All files were converted to.pdbqt format using AutoDockTools (ADT, version 1.5.7, https://autodock.scripps.edu/resources/adt/), and during this process, small molecule ligands, unnecessary metal ions, and other atoms were removed from the protein structure files. Molecular docking was then conducted using AutoDock Vina (version 1.1.2, https://vina.scripps.edu/), with the exhaustiveness set to 16 and other parameters kept at default settings. The conformations with the lowest binding energies from the docking results were visualized using PyMOL open-source version (version 2.6.0a0, https://pymol.org/2/).

Cell culture and cell model establishment

The H9c2 cells used in this study were obtained from Procell (Catalog No. CL-0089, China). Routine culture was performed in a medium composed of 89% Dulbecco's Modified Eagle Medium (with $NaHCO_3$ 1.5g/L) (iCell-128-001, Cellverse, China), 10% fetal bovine serum (10270–106, Gibco, Thermo Fisher Scientific, USA), and 1% penicillin/streptomycin (C0222, Beyotime, China), in an incubator at 37°C with 5% CO_2.

The oxygen and glucose deprivation (OGD) model was established following previous studies [22, 23]. Specifically, the medium was replaced with glucose-free medium, and the cells were placed in an incubator with 95% N_2 and 5% CO_2 (37°C) to create the ischemia-hypoxia model, simulating MI. After 6 hours, the cells showed reduced function, simulating HF. The glucose-free medium consisted of 89% glucose-free Dulbecco's Modified Eagle Medium (iCell-138-0001, Cellverse, China), 10% fetal bovine serum, and 1% penicillin/streptomycin.

Cell grouping and intervention

The final concentrations of the intervention compounds in the culture medium were as follows: 740 Y-P (CAS: 1236188-16-1, MCE, USA) at 12μM [24–26], Wortmannin (WTM) at 100 nM [27, 28]. The low dose of medioresinol (MDRN) (CAS: 40957-99-1, MCE, USA) is 60 μM, denoted as MDRN-L, and the high dose is 120 μM, denoted as MDRN-H. Cells were cultured under normal conditions for 48 hours, followed by 18 hours of drug intervention, and then

subjected to 6 hours of OGD treatment based on the drug intervention. The cells were divided into seven groups: the control group, the OGD model group, the OGD + 740 Y-P group (positive drug group), the OGD + WTM group, the OGD + MDRN-L group, the OGD + MDRN-H group, and the OGD + MDRN-H + WTM group.

Cell viability assay

Cell viability was measured using a commercially available CCK-8 assay kit (C0038, Beyotime, China) according to the manufacturer's instructions. This assay was used to evaluate the final drug concentrations and the extent of HF.

ELISA assays for NT-proBNP, TNF-α, and IL-1β

ELISA assays were conducted to measure N-terminal pro b-type natriuretic peptide (NT-proBNP), TNF-α, and IL-1β levels using commercially available kits: Rat NT-proBNP (20240408, DreamBio, China), Rat tumor necrosis factor-alpha (TNF-α) (20240427, DreamBio, China), and Rat interleukin-1 beta (IL-1β) (20240423, DreamBio, China). According to the manufacturer's instructions, NT-proBNP was measured using cell lysates, while TNF-α and IL-1β were measured using the culture supernatant.

Reactive oxygen species assay

Reactive oxygen species (ROS) levels were measured using a commercially available DCFH-DA ROS Detection Kit (S0033S, Beyotime, China). Specifically, after culturing the cells in a 96-well plate under OGD conditions for 4 hours, the detection reagent was quickly added, and the cells were further incubated under OGD conditions for another 2 hours. At the end of the incubation, ROS levels were directly measured using a Synergy H1 microplate reader (Bio-Tek, USA) with excitation at 488 nm and emission at 525 nm.

Mitochondrial membrane potential detection

Mitochondrial membrane potential was measured using a commercially available JC-1 Mitochondrial Membrane Potential Detection Kit (C2006, Beyotime, China). Cells were cultured in a 24-well plate, and after the culture period, the assay was performed according to the manufacturer's instructions. Images were captured using a Vert A1 inverted fluorescence microscope (Zeiss, Germany), and ImageJ software (version 1.54f) was used to analyze the average fluorescence intensity of the red and green fluorescence. Specifically, the integrated density of red fluorescence (R) was measured in the red channel, and the integrated density of green fluorescence (G) was measured in the green channel. The mitochondrial membrane potential depolarization was expressed as the ratio of green fluorescence intensity to the sum of red and green fluorescence intensities: $G/(R+G)$.

Western blot

Western blotting was performed according to standard protocols. The primary antibodies used were phosphatidylinositol 3-Kinase (PI3K) p110 alpha Monoclonal antibody (67071-1-Ig, Proteintech, China), Phospho- protein kinase B (AKT) Monoclonal antibody (66444-1-Ig, Proteintech, China), Phospho- mammalian target of rapamycin (mTOR) Monoclonal antibody (67778-1-Ig, Proteintech, China), and Alpha Tubulin Monoclonal antibody (66031-1-Ig, Proteintech, China). The dilution ratios were 1:1000, 1:2000, 1:2000, and 1:25000, respectively. A total of 40 μg of protein was loaded per sample.

The transfer was performed using a semi-dry transfer system. The membrane for phosphorylated mTOR (p-mTOR) and Tubulin was from a 6% gel, transferred at 25V for 40 minutes. The membrane for PI3Kα, phosphorylated AKT (p-AKT), and Tubulin was from a 10% gel, transferred at 25V for 15 minutes.

Imaging was performed using the Azure Sapphire RGBNIR imaging system, set to medium exposure intensity with automatic exposure. Band intensity was analyzed using ImageJ software.

All experimental data were statistically analyzed and visualized using GraphPad Prism 9 software (version 9.0.0, GraphPad Software, San Diego, CA, USA, https://www.graphpad.com/). The results are expressed as mean ± standard deviation. Comparisons between groups were performed using one-way analysis of variance (ANOVA) followed by Tukey's multiple comparison test. A p-value < 0.05 was considered statistically significant.

Results

Targets of components of Eucommiae cortex and their networks

From the database, 147 components of Eucommiae cortex were identified (S1 Table). Applying the screening criteria of OB > 30%, DL > 0.18, and MW < 500, 23 potential active components that may have good efficacy were selected (Table 1). Among them, CID21582571 does not have a corresponding CAS number, so its CID number is provided. GQNBCFQSSDOEHP-LNFBDUAVSA-N lacks both a CAS number and CID number, so its InChIKey is provided.

Among the 23 potential active components selected, two (GQNBCFQSSDOEHP-LNFB-DUAVSA-N and 32221-58-2) did not have their SMILES in PubChem. We used their structure files (.mol2) and converted them to SMILES using the Open Babel open-source tool (S1 File). Through the SWISS and TargetNet, we identified 627 potential targets for the potential active components of Eucommiae cortex using their SMILES. When uploaded to the DAVID database, it displayed 581 human targets and 46 targets from other species, resulting in 581 final targets. 22 out of these 23 compounds formed 1,513 connections with the 581 targets. (Fig 1, S2 Table). Among these, 288 connections had a binding probability greater than 0.5, shown as greenish lines in the figure, while connections with a probability less than 0.5 were shown in purplish colors. The nodes corresponding to compounds with higher DL are depicted in darker red, while those with lower DL are shown in lighter red.

Shared targets of HF, MI, and potential active components, and PPI network

We identified 136 shared targets (S3 Table). A PPI network was generated using these 136 shared targets (Fig 2A). Using the Molecular Complex Detection plugin in Cytoscape, four core clusters (Fig 2B–2E) were identified, comprising a total of 34 targets that cover multiple key biological processes. Core cluster 1 (Fig 2B) is primarily associated with matrix metalloproteinases (MMPs), estrogen receptors (ESR), and MAP kinase signaling pathways. Core cluster 2 (Fig 2C) is related to lipoxygenase (ALOX) and cyclooxygenase (COX) pathways. Core cluster 3 (Fig 2D) involves apoptosis, inflammatory response, and hypoxia response pathways, such as the AKT, mitogen-activated protein kinase (MAPK), and hypoxia-inducible factor 1 (HIF1) signaling pathways. Core cluster 4 (Fig 2E) focuses on the PI3K/AKT/mTOR signaling pathway. We further analyzed these 34 targets using CytoHubba and identified the top 15 proteins with the highest MCC score (Fig 2F) and the top 15 proteins with the highest Degree score (Fig 2G), with 12 proteins (S4 Table) being common between these metrics.

Table 1. 23 potential active components that may have good efficacy.

CAS/CID/Ichkey	Molecule Name	MW	OB (%)	DL
472-15-1	Mairin	456.78	55.37	0.77
573-44-4	liriodendrin_qt	450.48	53.13	0.79
13060-14-5	Yangambin	446.54	57.52	0.8
83-46-5	beta-sitosterol	414.79	36.91	0.75
4449-51-8	Cyclopamine	411.69	55.42	0.82
40957-99-1	(+)-medioresinol	388.45	87.18	0.61
526-06-7	(+)-Eudesmin	386.48	33.28	0.62
2955-23-9	olivil	376.44	62.22	0.4
81426-17-7	AIDS214634	374.42	92.42	0.54
CID21582571	(E)-3-[4-[(1R,2R)-2-hydroxy-2-(4-hydroxy-3-methoxy-phenyl)-1-methylol-ethoxy]-3-methoxy-phenyl]acrolein	374.42	56.31	0.36
GQNBCFQSSDOEHP-LNFBDUAVSA-N	Dehydrodiconiferyl alcohol 4,gamma'-di-O-beta-D-glucopyanoside_qt	358.42	51.44	0.39
4263-87-0	4-[(2S,3R)-5-[(E)-3-hydroxyprop-1-enyl]-7-methoxy-3-methyl-2,3-dihydrobenzofuran-2-yl]-2-methoxy-phenol	358.42	50.75	0.39
2134-98-7	(-)-Tabernemontanine	354.49	58.66	0.6
4423-37-4	Syringetin	346.31	36.82	0.37
32221-58-2	hirsutin_qt	345.35	49.81	0.37
4433-08-3	Dehydrodieugenol	326.42	30.1	0.23
572-59-8	Cinchonan-9-al, 6'-methoxy-, (9R)-	324.46	68.21	0.4
117-39-5	quercetin	302.25	46.43	0.27
466-77-3	Erythraline	297.38	49.17	0.55
83145-47-5	3-beta-Hydroxymethyllenetanshiquinone	294.32	32.16	0.4
35323-91-2	ent-Epicatechin	290.29	48.95	0.24
520-18-3	kaempferol	286.25	41.88	0.24
6754-13-8	Helenalin	262.33	77.01	0.19

MW, Molecular Weight; OB, Oral Bioavailability; DL, Drug-likeness

https://doi.org/10.1371/journal.pone.0311143.t001

These metrics help highlight proteins that may play crucial roles in the biological processes under study. A detailed comparison between the MCC and Degree results shows that despite their different calculation methods, the overlap of 12 common proteins underscores their potential significance as key regulators within the network.

KEGG and GO enrichment analysis of shared targets of disease and Eucommiae cortex components

The 136 shared targets identified in section "shared targets of HF, MI, and potential active components, and PPI network" were imported into the DAVID database for KEGG and GO enrichment analysis. We obtained 98 KEGG pathways, 70 GOBP terms, 17 GOCC terms, and 32 GOMF terms (S5 Table). These data represent an overview of the potential functions that the potential active components of Eucommiae cortex could achieve through MI and HF-related target proteins.

As shown in Fig 3A, the KEGG pathways mainly involve processes such as cancer signaling, microRNA regulation, calcium signaling, lipid metabolism and atherosclerosis, neutrophil extracellular trap formation, angiogenesis, inflammation, and oxidative stress. Among these, pathways such as calcium signaling, lipid metabolism and atherosclerosis, hypoxia-inducible factor 1 (HIF-1) signaling, and vascular endothelial growth factor signaling are significantly
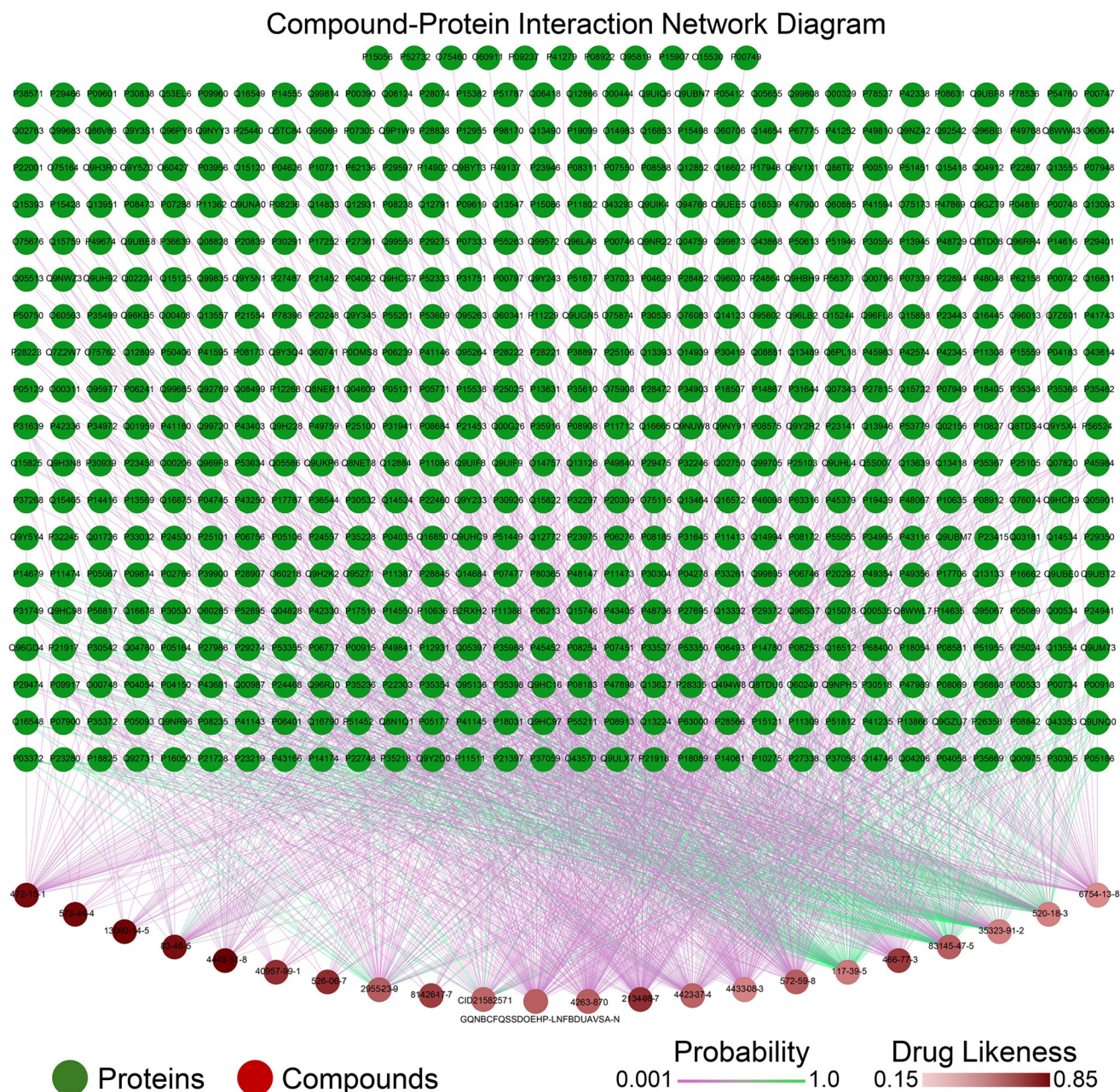
Fig 1. The interaction network diagram of 22 compounds and 581 targets. Green nodes represent proteins, and red nodes represent compounds. The edges connecting these nodes indicate predicted interactions between specific compounds and proteins, with the color of the edges reflecting the probability of interaction; green edges indicate higher probability, while purple edges indicate lower probability. The intensity of the red color in the compound nodes represents the drug-likeness score, with darker red indicating higher drug-likeness.

associated with cardiovascular diseases. These pathways play crucial roles in myocardial contraction, vascular tone regulation, inflammatory response, oxidative stress, and angiogenesis, which are key mechanisms in the occurrence and development of cardiovascular diseases.

As shown in Fig 3B, the GO biological process enrichment analysis primarily involves processes such as protein phosphorylation, adenosine triphosphate binding, the formation and
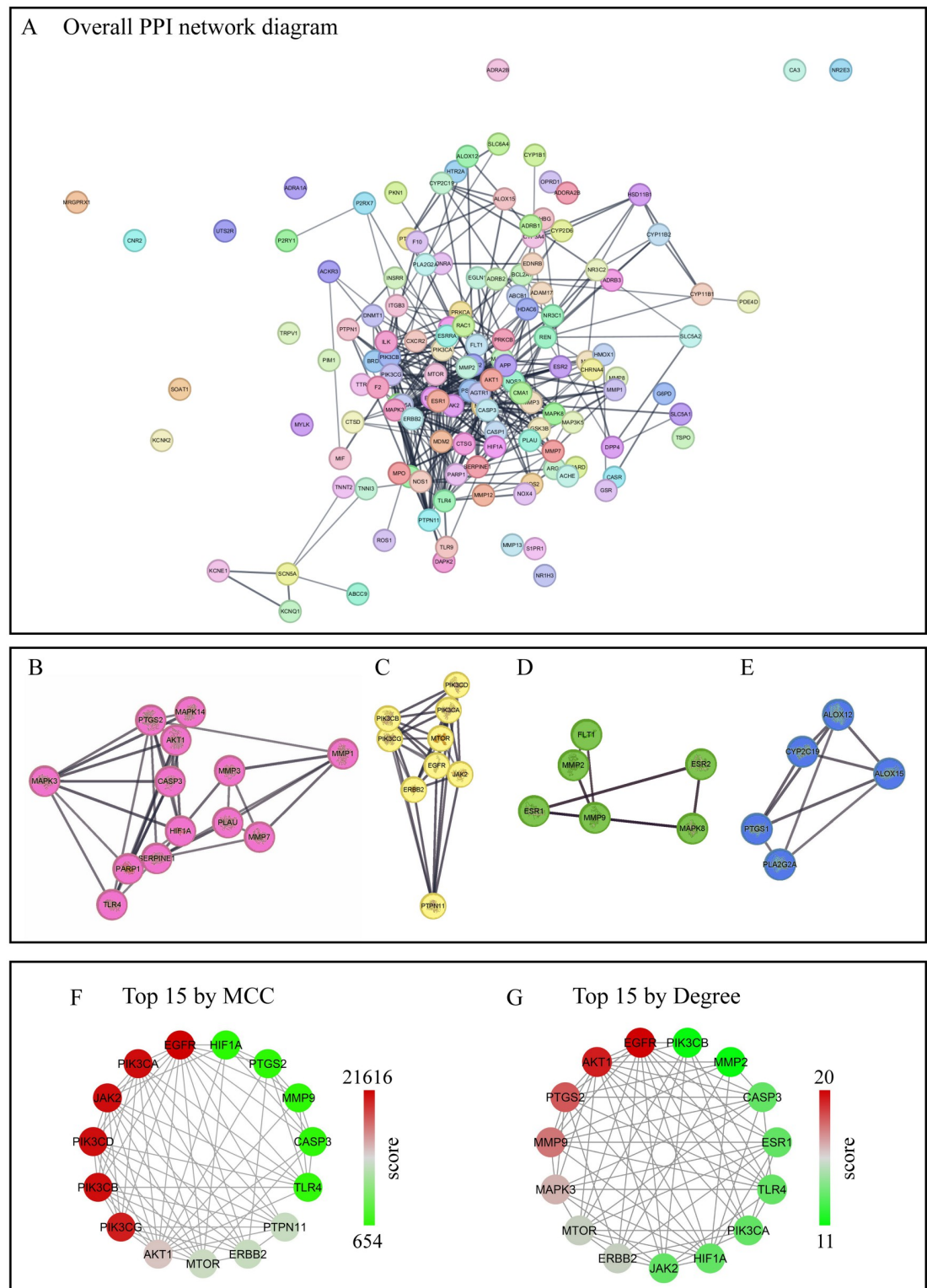
Fig 2. The PPI network diagram of 136 shared proteins. (**A**), The overall PPI network diagram of 136 shared proteins. (**B**)-(**E**), The four core clusters identified using the Molecular Complex Detection plugin in Cytoscape, shown individually. (**F**), The PPI network of the top 15 proteins by MCC. These proteins are part of highly interconnected subnetworks (cliques) within the PPI network. (**G**), The PPI network of the top 15 proteins by Degree. These proteins are key hubs in the PPI network. As in (**F** and **G**), nodes are colored based on their Degree or MCC scores, with red indicating more higher scores. In all panels (**A**)-(**G**), targets are labeled with their name abbreviations. PPI, Protein-Protein Interaction; MCC, Maximal Clique Centrality.

https://doi.org/10.1371/journal.pone.0311143.g002
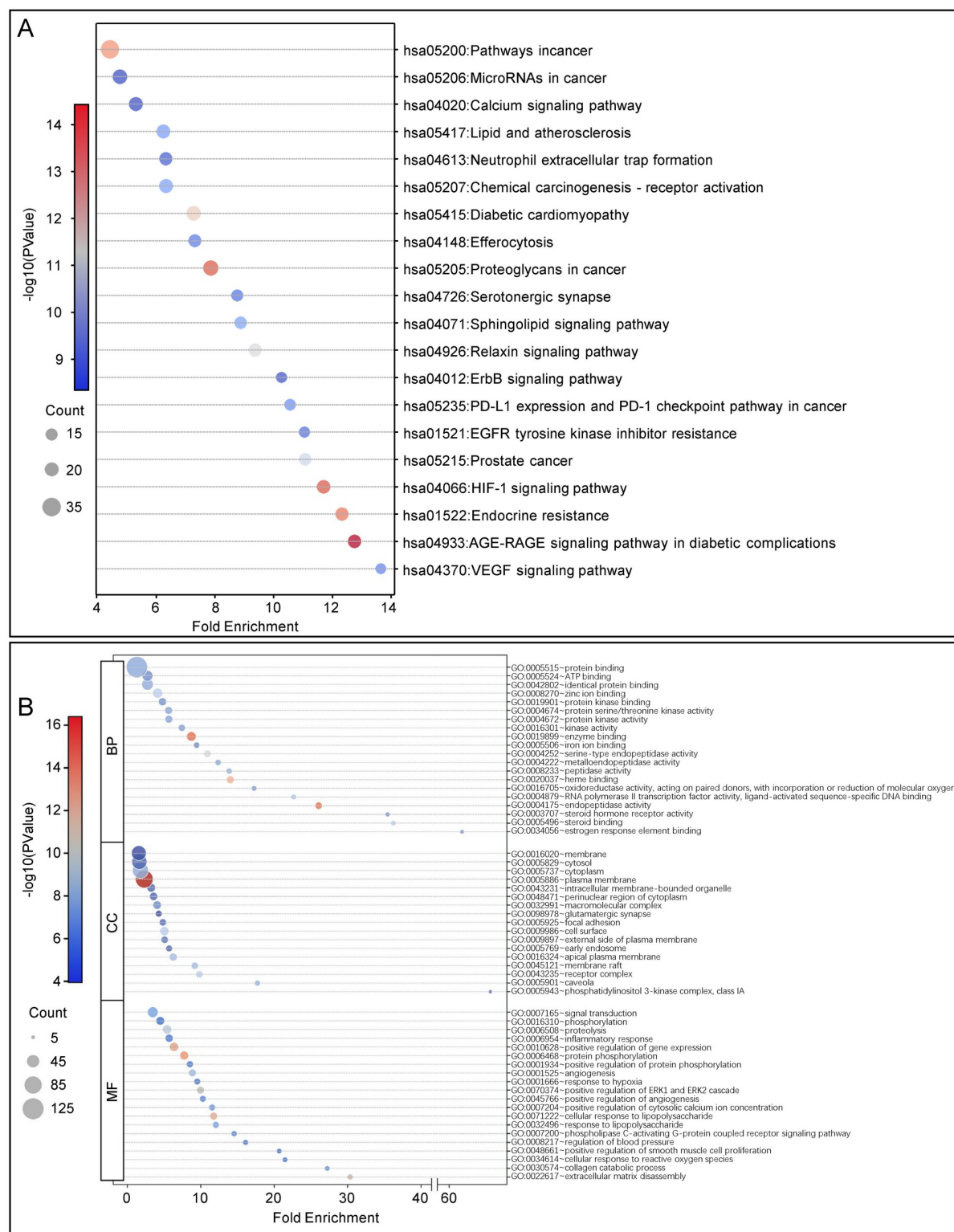
Fig 3. The KEGG and GO enrichment analysis of 136 shared proteins. (**A**) top 20 KEGG enriched based on p-value. The x-axis represents the fold enrichment, which indicates the degree of enrichment for each pathway, and the y-axis lists the names of the pathways. The size of the dots corresponds to the "count," which is the number of proteins associated with each pathway, and the color gradient represents the -log10(p-value), indicating the significance of the enrichment. (**B**) top 20 GO enriched based on p-value. The x-axis represents the fold enrichment, indicating the degree of enrichment for each GO term, and the y-axis lists the specific GO terms categorized into Biological

Process (BP), Cellular Component (CC), and Molecular Function (MF). The size of the dots corresponds to the "count," which is the number of proteins associated with each GO term, and the color gradient represents the -log10(p-value), showing the significance of the enrichment. KEGG, Kyoto Ency-clopedia of Genes and Genomes; GO, Gene Ontology; BP, Biological Process; CC, Cellular Component; MF, Molecular Function.

https://doi.org/10.1371/journal.pone.0311143.g003

function of protein complexes, metal ion binding, and redox reactions. Pathways significantly related to cardiovascular diseases include the response to lipopolysaccharide, inflammatory response, angiogenesis, and response to hypoxia. These pathways play important roles in regulating vascular function, immune response, and cell survival [29–31]. In the GO cellular component enrichment analysis, the main cellular structures involved are the cell membrane, cytoplasm, extracellular matrix, and signaling complex. These structures are crucial in intercellular signal transduction, substance transport, and the maintenance of the intra- and extracellular environment. Pathways related to cardiovascular diseases mainly include the early endosome, perinuclear region, and extracellular matrix composition, which affect cellular functions and the stability of tissue structures [32, 33]. In the GO molecular function enrichment analysis, the primary functions involved are protein binding, enzyme binding, metal ion binding, and oxidoreductase activity. These molecular functions play significant roles in protein-protein interactions, enzyme regulation, and the maintenance of cellular redox states. Pathways significantly related to cardiovascular diseases include protein phosphorylation, enzyme binding, and redox reactions, influencing cellular signal transduction and metabolic processes [34, 35].

Through the above analyses, it can be preliminarily confirmed that the effective components of Eucommia exert effects related to oxidative stress and inflammatory responses associated with MI and HF.

Key proteins highly expressed in myocardium and key KEGG pathways and key GO terms

Key proteins with enriched expression in the myocardium were identified by screening using the Genomics Institute of the Novartis Research Foundation and the Human Protein Atlas. Each source identified six proteins (S6 Table) from the set of 12 key proteins identified in the results of section "shared targets of HF, MI, and potential active components, and PPI network". By intersecting the two sets, five proteins with enriched expression in the myocardium were obtained (Table 2).

Using the five critical proteins identified in the myocardium in Table 2, KEGG and GO enrichment analyses were performed. This resulted in the identification of 22 KEGG pathways, 8 GOBP, 0 GOCC, and 3 GOMF (S7 Table). The connections between the five proteins and these pathways were visualized (Fig 4). The 22 identified KEGG pathways encompass various

**Table 2. 5 targets highly expressed in myocardial tissue.**

UNIPROT ID	GENE NAME
P31749	AKT serine/threonine kinase 1(AKT1)
O60674	Janus kinase 2(JAK2)
P04626	erb-b2 receptor tyrosine kinase 2(ERBB2)
P42345	mechanistic target of rapamycin kinase(MTOR)
P42336	phosphatidylinositol-4,5-bisphosphate 3-kinase catalytic subunit alpha(PIK3CA)

These 5 protein targets are the highest expressed in myocardial tissue among the 12 key proteins.

https://doi.org/10.1371/journal.pone.0311143.t002

Target-KEGG/GO Network Diagram
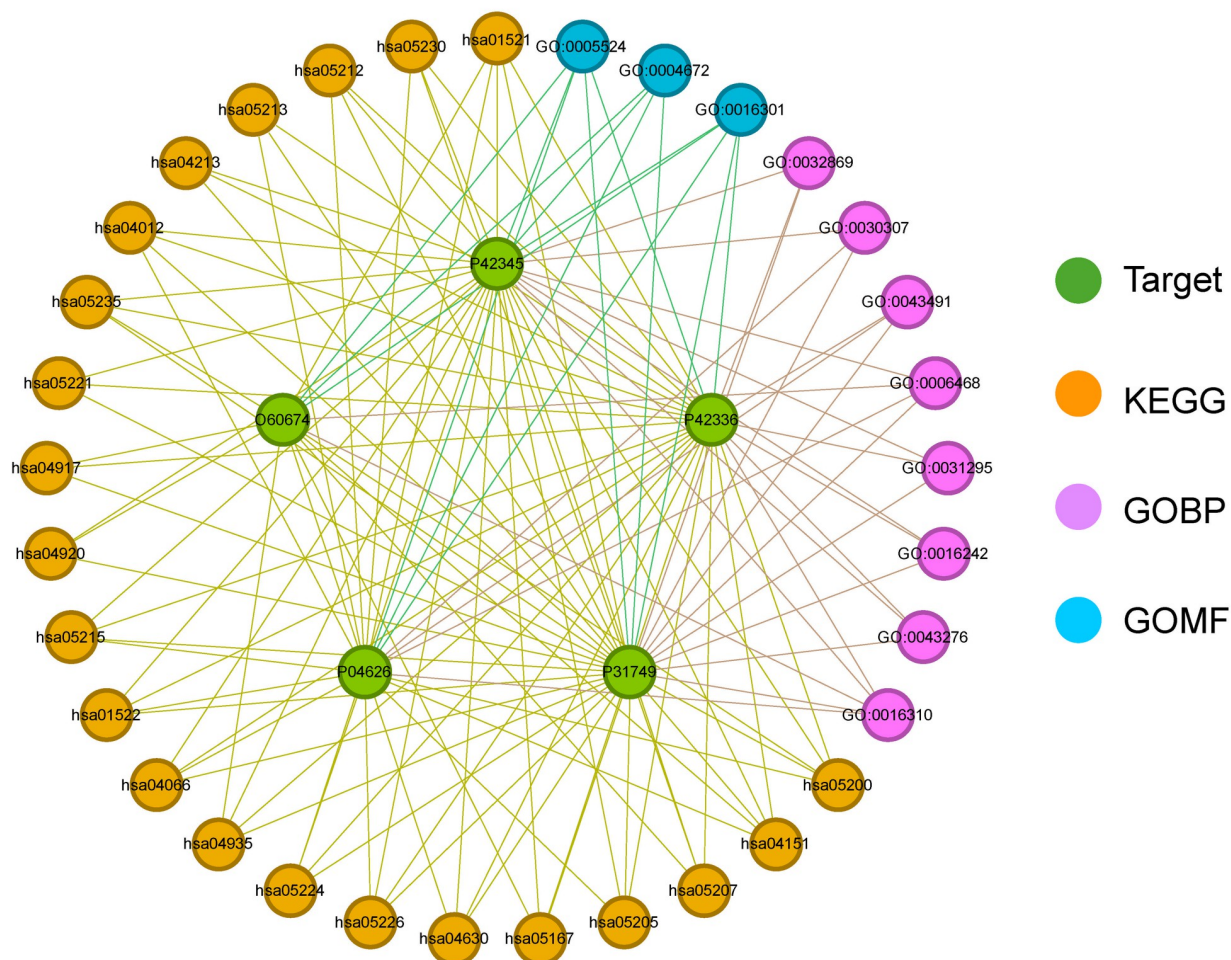
hsa01521:EGFR tyrosine kinase inhibitor resistance
hsa01522:Endocrine resistance
hsa04012:ErbB signaling pathway
hsa04066:HIF-1 signaling pathway
hsa04151:PI3K-Akt signaling pathway
hsa04213:Longevity regulating pathway-multiple species
hsa04630:JAK-STAT signaling pathway
hsa04917:Prolactin signaling pathway
hsa04920:Adipocytokine signaling pathway
hsa04935:Growth hormone synthesis, secretion and action
hsa05167:Kaposi sarcoma-associated herpesvirus infection
hsa05200:Pathways in cancer
hsa05205:Proteoglycans in cancer
hsa05207:Chemical carcinogenesis-receptor activation
hsa05212:Pancreatic cancer
hsa05213:Endometrial cancer
hsa05215:Prostate cancer

hsa05221:Acute myeloid leukemia
hsa05224:Breast cancer
hsa05226:Gastric cancer
hsa05230:Central carbon metabolism in cancer
hsa05235:PD-L1 expression and PD-1 checkpoint pathway in cancer
GO:0004672~protein kinase activity
GO:0005524~ATP binding
GO:0006468~protein phosphorylation
GO:0016242~negative regulation of macroautophagy
GO:0016301~kinase activity
GO:0016310~phosphorylation
GO:0030307~positive regulation of cell growth
GO:0031295~T cell costimulation
GO:0032869~cellular response to insulin stimulus
GO:0043276~anoikis
GO:0043491~protein kinase B signaling

Fig 4. The KEGG and GO enrichment analysis of 5 highly expressed targets in myocardial tissue. Labels in the diagram are represented by KEGG and GO identifiers, as well as the UniProt IDs of target proteins. KEGG, Kyoto Encyclopedia of Genes and Genomes; GOBP, Gene Ontology Biological Process; GOMF, Gene Ontology Molecular Function.

https://doi.org/10.1371/journal.pone.0311143.g004

biological processes, including cancer-related signaling, metabolic regulation, cell survival and proliferation, and immune responses. Among these pathways, the PI3K/Akt signaling pathway, HIF-1 signaling pathway, Janus kinase/signal transducer and activator of transcription (JAK-STAT) signaling pathway, and Prolactin signaling pathway are known to be closely related to MI and HF and are thus highlighted as key pathways of interest [36–38]. The identified GO terms cover important biological processes and molecular functions such as phosphorylation, apoptosis, autophagy regulation, T cell co-stimulation, cell growth regulation, and insulin response. These processes and functions are closely related to cardiovascular diseases, particularly MI and HF. For example, phosphorylation and protein kinase activity play crucial roles in the regulation of cardiomyocyte function [39] and signal transduction; anoikis and autophagy regulation affect the survival of cardiomyocytes [40, 41].

Overall network of Eucommiae cortex in treating MI and HF

The final key proteins, key KEGG pathways, GO terms, and corresponding potential active components of Eucommia were matched and combined with the diseases to create a compound-target-KEGG/GO-disease network diagram (Fig 5). Ultimately, 13 compounds from Eucommia were found to act on 5 key targets, influencing MI and HF through 22 major KEGG pathways and 11 major GO terms (including 8 GOBP, 0GOCC, and 3 GOMF).

## Key PI3K/AKT/mTOR targets in Eucommia cortex components revealed by molecular docking

We selected 13 effective components of Eucommia and 5 target proteins in the entire network, performing molecular docking on their 18 connections to evaluate their binding stability. As shown in Fig 6, the binding modes with the lowest binding energy for the 18 dockings are presented. The heatmap shows the variations in the lowest binding energies, with the highest being -4.2 kcal/mol for the binding of 6754-13-8 with O60674, and the lowest being -10.8 kcal/mol for the binding of 2134-98-7 with P42345. Compounds with a greener background color have higher drug-likeness, whereas those with a less green background have lower drug-likeness. The figure shows that in the molecular dockings of the compounds with higher DL values (numbered 2, 7, 8, 14, 16, and 17), they all bind with PI3K, AKT, and mTOR. This indicates that the three key proteins in the PI3K/AKT/mTOR pathway are targets for the effective components of Eucommia. We aim to choose the most upstream PI3K as the target, and further validate through cell experiments whether the effective components of Eucommia can activate downstream AKT/mTOR by regulating PI3K, thereby improving MI and HF. In selecting the components, we will choose those that only act on PI3K and have higher DL values. This points to the compound with CAS number 40957-99-1, commonly known as medioresinol.

MDRN alleviates OGD-induced damage via PI3K/AKT/mTOR pathway

After incubating cells with various concentrations of MDRN for 24 hours, we observed significant cell death at concentrations greater than 120 μM (S1 Fig). Therefore, we selected 120 μM as the final intervention concentration. A concentration of 60 μM was used as the low-dose intervention group.

As shown in Fig 7A and 7B, the OGD model cells exhibited reduced viability and elevated NT-proBNP levels, indicating successful construction of a HF induced by OGD model. Inhibiting PI3Kα with WTM exacerbated these effects, whereas the PI3Kα agonist 740 Y-P improved them. Similarly, MDRN was able to counteract OGD-induced damage. The protective effect of MDRN was attenuated when PI3K was inhibited with WTM. However, cell viability remained higher than in the OGD+WTM group, and NT-proBNP levels were lower than
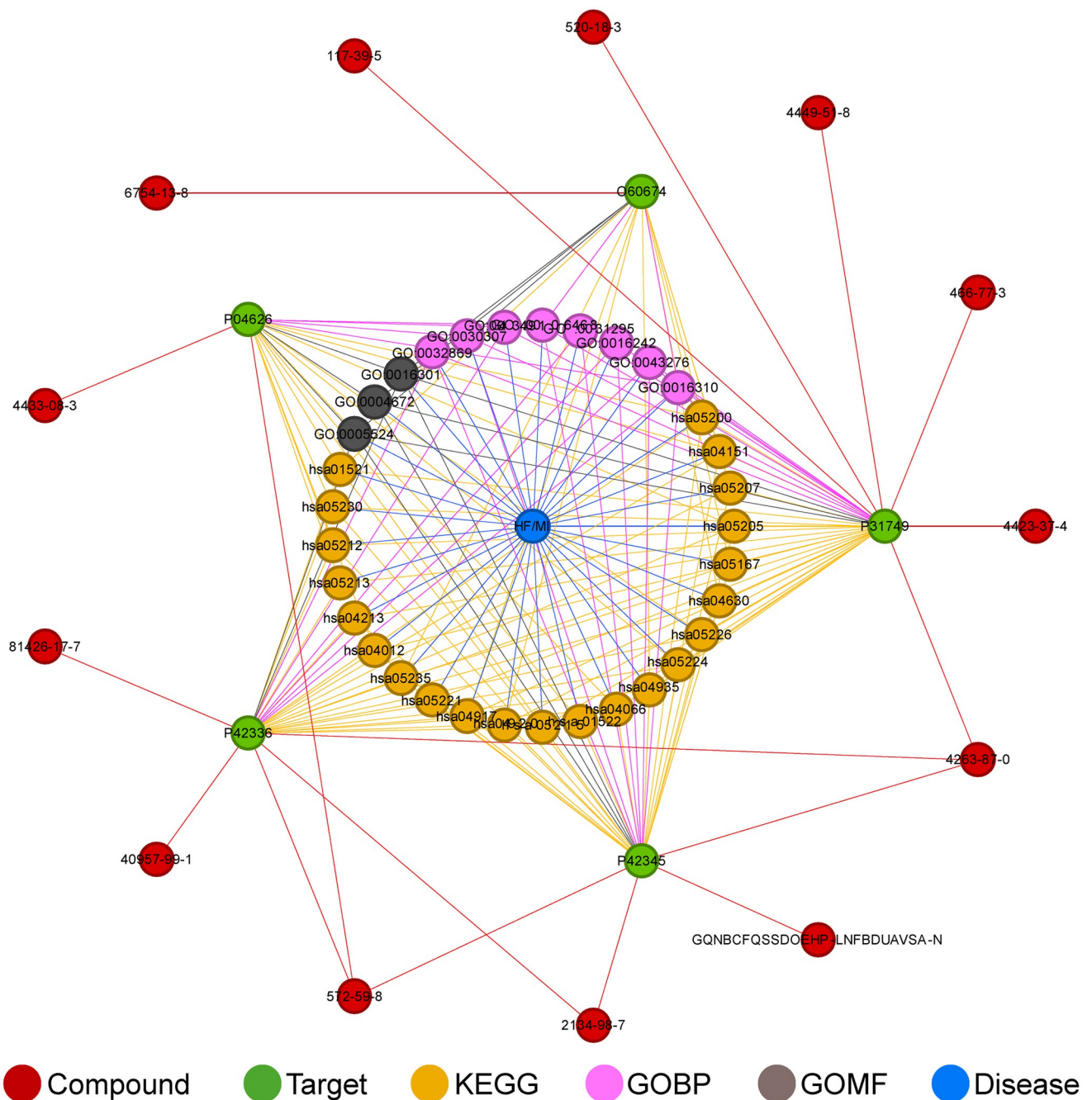
Fig 5. The overall network diagram of myocardial highly expressed targets mediating the effects of Eucommia's potential active components on KEGG/GO and disease. Labels in the diagram are represented by KEGG and GO identifiers, UniProt IDs of target proteins, and CAS numbers or Ichkey of compounds. HF, heart failure; MI, myocardial infarction; KEGG, Kyoto Encyclopedia of Genes and Genomes; GOBP, Gene Ontology Biological Process; GOMF, Gene Ontology Molecular Function.

in the OGD+WTM group. This suggests that PI3K is an effective target for MDRN in improving post-MI HF, though not the sole target. Furthermore, this effect is concentration-dependent, with suboptimal effects observed at lower concentrations of MDRN.

Similarly, in oxidative stress (Fig 7C) and inflammatory responses (Fig 7D and 7E), the OGD model showed more severe conditions compared to the control group, characterized by
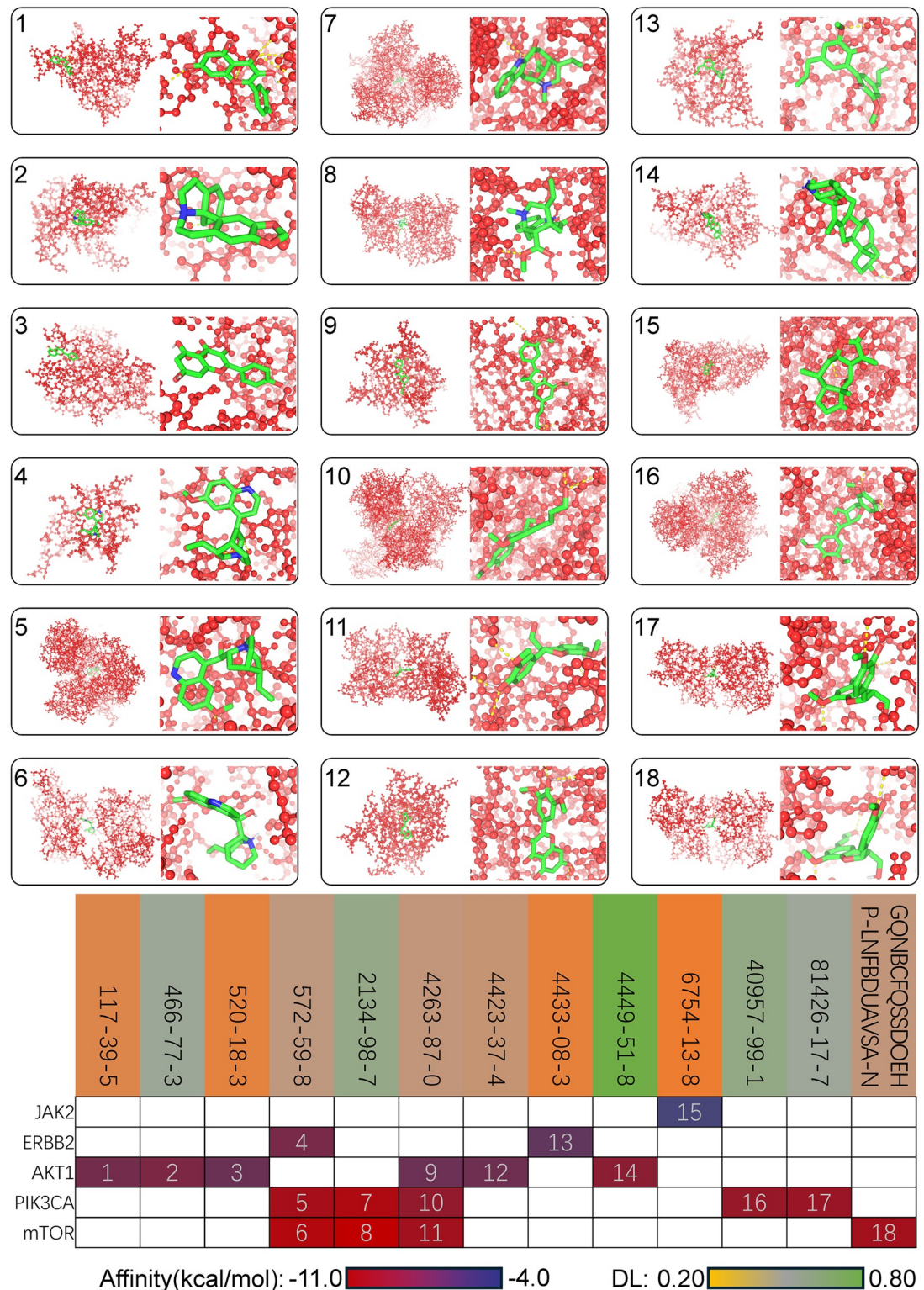
Fig 6. Molecular docking diagrams of 18 types of interactions among compound targets and the heatmap of the lowest binding energy for each interaction. The numbers in the top left corner of the molecular docking diagrams correspond to the numbers in the heatmap. Compounds are labeled with their CAS numbers or Ichkey, and proteins are labeled with gene name abbreviations. DL, drug likeness.

https://doi.org/10.1371/journal.pone.0311143.g006
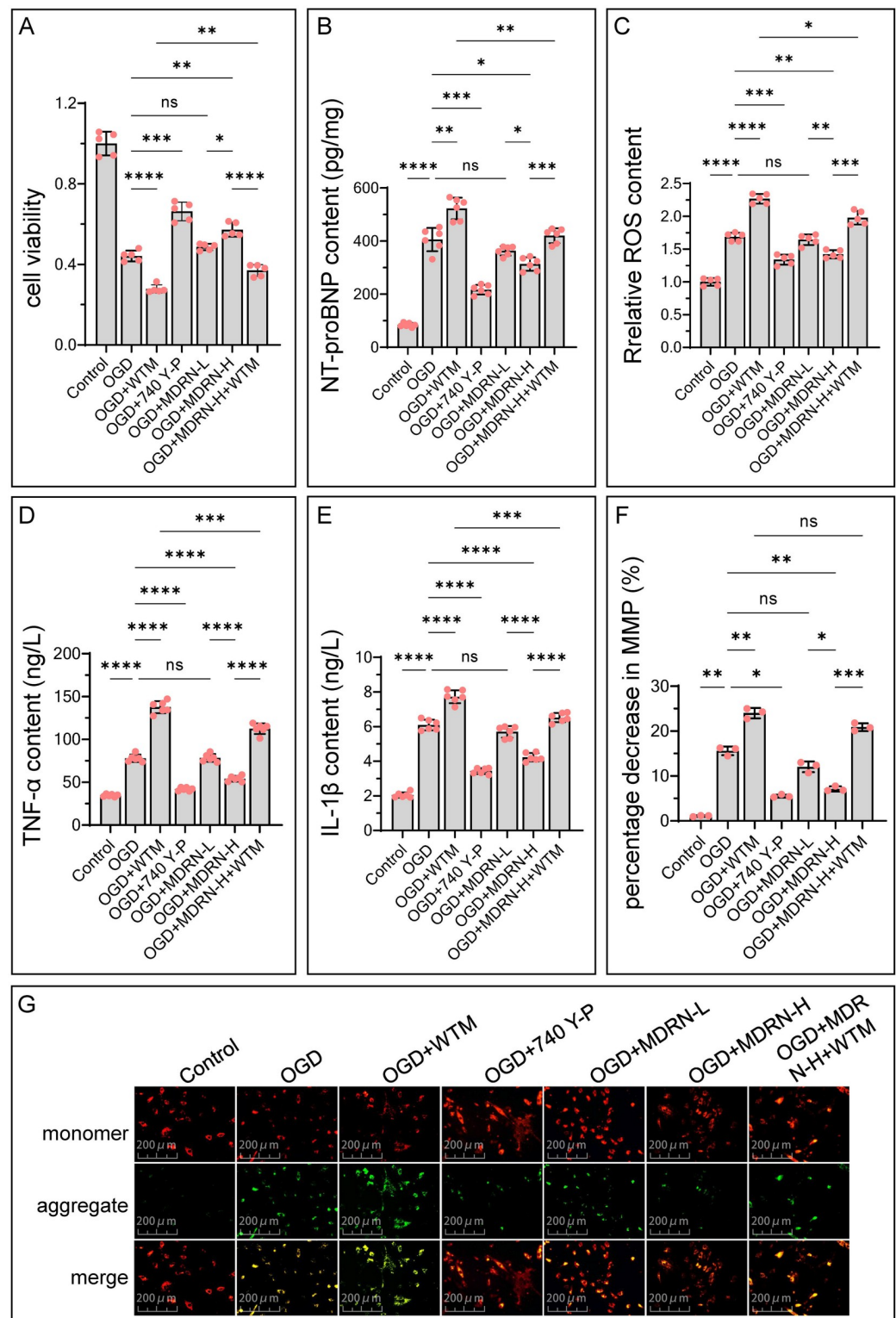
Fig 7. The conditions of heart failure, oxidative stress, inflammatory response, and mito-chondrial membrane potential in each group of cells. (**G**) Displays images under a fluorescence microscope after JC-1 staining. Each (red circle) represents a sample data point. ns $p \geq 0.05$, *$p < 0.05$, **$p < 0.01$, ***$p < 0.001$, ****$p < 0.0001$. NT-proBNP, N-terminal pro b-type Natriuretic Peptide; ROS, Reactive Oxygen Species; TNF-α, Tumor Necrosis Factor-alpha; IL-1β, Interleukin-1 beta; MMP, Mitochondrial Membrane Potential; OGD, Oxygen and Glucose Deprivation; WTM, Wortmannin; MDRN, Medioresinol; L, Low Dose; H, High Dose.

significantly elevated levels of ROS, TNF-α, and IL-1β. Following MDRN treatment, ROS, TNF-α, and IL-1β levels were markedly reduced. However, the therapeutic effect of MDRN was diminished when PI3Kα was inhibited. Cardiomyocytes contain abundant mitochondria, and their function is closely related to mitochondrial activity, reflected by mitochondrial membrane potential, which can indicate oxidative stress levels effectively. As shown in Fig 7F and 7G, JC-1 mitochondrial staining fluorescence images demonstrated that OGD caused a decrease in mitochondrial membrane potential. Specific inhibition of PI3Kα further reduced mitochondrial membrane potential, while activation restored it. MDRN, similar to a PI3K activator, effectively restored mitochondrial membrane potential, which was attenuated by PI3Kα inhibitors.

Oxidative stress and inflammatory responses are regulatory targets of the PI3Kα-AKT-mTOR pathway. As shown in Fig 8, compared to the control group, the OGD group exhibited varying degrees of reduction in PI3K, p-AKT, and p-mTOR levels. Following MDRN treatment, there was a recovery in PI3K, p-AKT, and p-mTOR levels compared to the OGD group. However, inhibition of PI3K reduced the extent of MDRN-induced recovery of p-AKT and p-mTOR. Therefore, MDRN's improvement in MI and HF is closely related to the PI3K/AKT/mTOR pathway, with PI3K being a key target for MDRN to activate this pathway.

Discussion

This study systematically explored the potential therapeutic effects and mechanisms of Eucommiae cortex in the treatment of HF following MI. Utilizing network analysis and molecular docking approaches, we screened and analyzed the potential active compounds of Eucommiae cortex, and validated their anti-inflammatory and antioxidant properties of MDRN through in vitro experiments. Specifically, 23 potential active compounds were identified from the database using stringent criteria (OB ≥ 30%, DL ≥ 0.18, and MW < 500) to ensure high drug potential. Out of the predicted 581 potential targets, 136 targets were found to be associated with HF and MI through PPI. KEGG, and GO enrichment analyses, indicating that Eucommiae cortex may exert its effects through pathways such as PI3K/AKT/mTOR, HIF-1, and JAK-STAT, which are involved in calcium signaling, lipid metabolism, inflammatory response, and oxidative stress. The PI3K/AKT/mTOR, HIF-1, and JAK-STAT pathways play crucial roles in cellular processes relevant to cardiovascular health, particularly in the context of MI and HF. The PI3K/AKT/mTOR pathway is pivotal for cellular growth, proliferation, and survival, and has been shown to enhance cardiac function by promoting angiogenesis, reducing apoptosis, and improving mitochondrial function, thereby mitigating damage from MI and HF [42]. The HIF-1 pathway, activated in response to hypoxia, supports cellular adaptation to low oxygen levels by promoting angiogenesis and metabolic adjustments, which improve tissue survival and function during MI [43, 44]. The JAK-STAT pathway, integral to inflammatory and cellular stress responses, has emerged as a critical target in cardiovascular diseases associated with autoimmune disorders. Research has indicated that JAK-STAT signaling contributes to inflammation and cardiovascular risk, and its inhibitors may offer new treatment strategies [45]. These pathways collectively contribute to essential mechanisms like oxidative stress regulation, lipid metabolism, calcium signaling, and inflammatory responses, which are vital for cardiovascular health.

Molecular docking analysis indicated that the selected compounds could stably bind to their targets, especially PI3K, AKT, and mTOR. We chose MDRN, which acts on the PI3K/Akt/mTOR pathway, for in-depth study and validated its effects on MI-induced HF through in vitro experiments. The results showed that MDRN could significantly improve oxidative stress and inflammatory response in myocardial ischemia-hypoxia model cells by activating
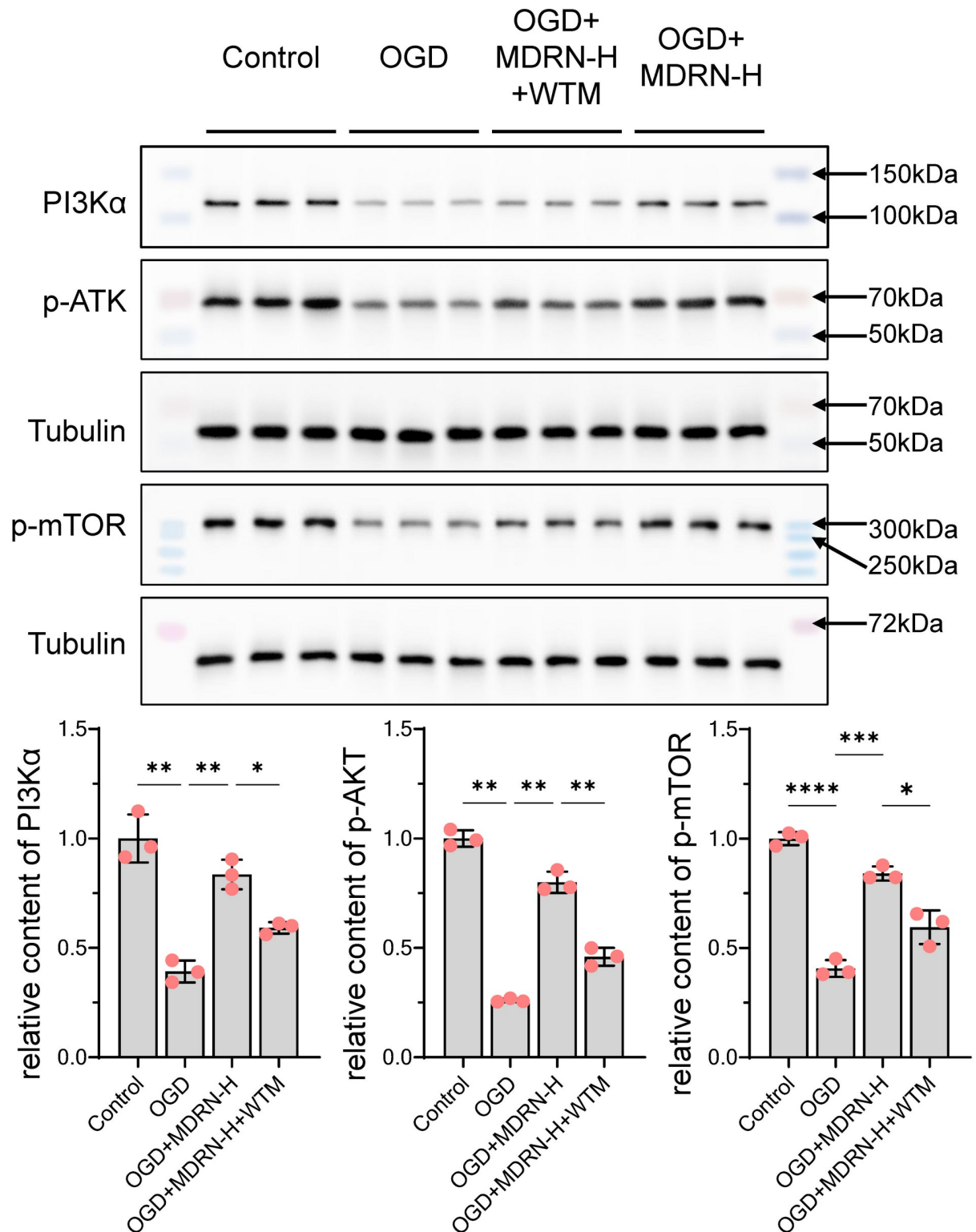
Fig 8. The Western blot detection results of PI3K, p-AKT, and p-mTOR. Each (red circle) represents a sample data point. ns $p \geq 0.05$, *$p < 0.05$, **$p < 0.01$, ***$p < 0.001$, ****$p < 0.0001$. OGD, Oxygen and Glucose Deprivation; WTM, Wortman-nin; MDRN-H, High Dose Medioresinol; PI3Kα, Phosphoinositide 3-kinase alpha; p-AKT, Phosphorylated Protein Kinase B; p-mTOR, Phosphorylated Mechanistic Target of Rapamycin.

the PI3K/AKT/mTOR signaling pathway, enhancing cell viability and mitochondrial membrane potential. This is consistent with previous studies that have also demonstrated that activating the PI3K/AKT/mTOR pathway can reduce cell apoptosis, improve mitochondrial function, and enhance overall cell survival under ischemic conditions [46]. This study not only confirms the role of the PI3K/AKT/mTOR pathway in the cardiovascular protective effects of Eucommiae cortex but also provides specific cellular-level regulatory evidence, offering a theoretical basis for the treatment of MI-induced HF with Eucommiae cortex.

Medioresinol, a lignan compound found in flaxseed and Eucommiae cortex, is known for its antioxidant, anti-inflammatory, and anticancer properties. Current research on MDRN is limited. It has been shown that brain microvascular endothelial cells undergo pyroptosis after ischemic stroke, and MDRN, as a peroxisome proliferator-activated receptor gamma coactivator 1-alpha activator, ameliorates pyroptosis and ischemic brain injury by reducing mitochondrial ROS via the peroxisome proliferator-activated receptor alpha/glutamate oxaloacetate transaminase 1 axis [47]. Another study found that MDRN leads to ROS accumulation in fungi [48]. Our research further supports that MDRN reduces oxidative stress post-ischemia. The anti-inflammatory effects of lignans and their metabolites are well-documented [49], but there are no direct studies on the anti-inflammatory effects of MDRN. Our study is the first to demonstrate through in vitro experiments that MDRN can inhibit ischemia-induced inflammatory responses, reducing TNF-α and IL-1β levels.

However, this study has certain limitations. Firstly, the single compound MDRN cannot fully represent the entire spectrum of Eucommiae cortex's therapeutic functions. Secondly, due to budget constraints, this research was limited to in vitro experiments. Therefore, we plan to conduct further studies to validate the overall efficacy and mechanisms of Eucommiae cortex in treating MI-induced HF, using both animal models and cell models to explore the therapeutic effects and molecular mechanisms of Eucommiae cortex and its compounds.

Conclusions

This study utilized network analysis and molecular docking to systematically analyze the potential targets and mechanisms of Eucommiae cortex in MI-induced HF, and validated its anti-inflammatory and antioxidant capabilities through in vitro experiments. The findings suggest that the active compound MDRN may exert therapeutic effects on MI-induced HF by activating the PI3K/AKT/mTOR signaling pathway, inhibiting inflammatory response, and reducing oxidative stress, thus improving mitochondrial membrane potential. These results provide a new theoretical foundation and research direction for the application of Eucommiae cortex in the treatment of cardiovascular diseases. Future research should aim to further promote the application and development of Eucommiae cortex in cardiovascular disease treatment.

Supporting information

S1 Table. 147 components of Eucommia cortex from TCMSP.
(XLSX)

S2 Table. The 1513 connections formed between the 22 compounds and 581 targets.
(XLSX)

S3 Table. The 136 shared targets between the disease and compounds and their UniProt IDs.
(XLSX)

S4 Table. The 12 shared targets identified by both MCC and degree analysis.
(XLSX)

S5 Table. KEGG and GO enrichment tables for the 136 shared targets between the disease and compounds.
(XLSX)

S6 Table. Six myocardial highly expressed proteins screened through the GNF and six myocardial highly expressed proteins screened through the HPA.
(XLSX)

S7 Table. KEGG and GO enrichment tables for the 5 key proteins jointly screened by GNF and HPA.
(XLSX)

S1 Fig. CCK-8 assay to determine the cell viability of H9c2 cells cultured with different concentrations of MDRN for 24 hours.
(PDF)

S1 File. Two compounds (GQNBCFQSSDOEHP-LNFBDUAVSA-N and 32221-58-2) and their SMILES obtained through conversion.
(ZIP)

S1 Raw images.
(PDF)

Author Contributions

Conceptualization: Qiyao Xu.

Data curation: Xueting Qin, Xuan Liu.

Formal analysis: Xuan Liu.

Methodology: Xueting Qin, Qiyao Xu.

Project administration: Xueting Qin.

Software: Xuan Liu, Can Guo.

Supervision: Qiyao Xu.

Validation: Xueting Qin, Li Huang.

Visualization: Xuan Liu, Qiyao Xu.

Writing – original draft: Xueting Qin, Xuan Liu.

Writing – review & editing: Can Guo, Li Huang, Qiyao Xu.

References

1. Zhang S, Zhao D, Yang Z, Wang F, Yang S, Wang C. Circulating mitochondria promoted endothelial cGAS-derived neuroinflammation in subfornical organ to aggravate sympathetic overdrive in heart failure mice. J Neuroinflammation. 2024; 21:27. https://doi.org/10.1186/s12974-024-03013-x PMID: 38243316

2. Weissman D, Maack C. Redox signaling in heart failure and therapeutic implications. Free Radic Biol Med. 2021; 171:345–64. https://doi.org/10.1016/j.freeradbiomed.2021.05.013 PMID: 34019933

3.   Petrie JR, Guzik TJ, Touyz RM. Diabetes, Hypertension, and Cardiovascular Disease: Clinical Insights and Vascular Mechanisms. Can J Cardiol. 2018; 34:575–84. https://doi.org/10.1016/j.cjca.2017.12.005 PMID: 29459239

4.   Bozkurt B, Aguilar D, Deswal A, Dunbar SB, Francis GS, Horwich T, et al. Contributory Risk and Management of Comorbidities of Hypertension, Obesity, Diabetes Mellitus, Hyperlipidemia, and Metabolic Syndrome in Chronic Heart Failure: A Scientific Statement From the American Heart Association. Circulation. 2016; 134:e535–535e578. https://doi.org/10.1161/CIR.0000000000000450 PMID: 27799274

5.   van Essen BJ, Voors AA, Tromp J. Risk factors for the development of heart failure in patients with or without prior myocardial infarction. Eur J Heart Fail. 2022; 24:985–7. https://doi.org/10.1002/ejhf.2538 PMID: 35560757

6.   Lenselink C, Ricken K, Groot HE, de Bruijne TJ, Hendriks T, van der Harst P, et al. Incidence and predictors of heart failure with reduced and preserved ejection fraction after ST-elevation myocardial infarction in the contemporary era of early percutaneous coronary intervention. Eur J Heart Fail. 2024. https://doi.org/10.1002/ejhf.3225 PMID: 38576163

7.   Canty JM Jr. Myocardial injury, troponin release, and cardiomyocyte death in brief ischemia, failure, and ventricular remodeling. Am J Physiol Heart Circ Physiol. 2022; 323:H1–1H15. https://doi.org/10.1152/ajpheart.00093.2022 PMID: 35559722

8.   McDonagh TA, Metra M, Adamo M, Gardner RS, Baumbach A, Böhm M, et al. 2023 Focused Update of the 2021 ESC Guidelines for the diagnosis and treatment of acute and chronic heart failure. Eur Heart J. 2023; 44:3627–39. https://doi.org/10.1093/eurheartj/ehad195 PMID: 37622666

9.   Carberry J, Marquis-Gravel G, O'Meara E, Docherty KF. Where Are We With Treatment and Prevention of Heart Failure in Patients Post-Myocardial Infarction. JACC Heart Fail. 2024: S2213–1779(24)00410-4 [pii]. https://doi.org/10.1016/j.jchf.2024.04.025 PMID: 38878010

10.   Wang S, Yu X, Wu S, Yang W, Gao Y, Wang W, et al. Simultaneous determination of periplocin, periplocymarin, periplogenin, periplocoside M and periplocoside N of Cortex Periplocae in rat plasma and its application to a pharmacokinetic study. Biomed Chromatogr. 2022; 36:e5283. https://doi.org/10.1002/bmc.5283 PMID: 34816469

11.   Huang Q, Zhang F, Liu S, Jiang Y, Ouyang D. Systematic investigation of the pharmacological mechanism for renal protection by the leaves of Eucommia ulmoides Oliver using UPLC-Q-TOF/MS combined with network pharmacology analysis. Biomed Pharmacother. 2021; 140:111735. https://doi.org/10.1016/j.biopha.2021.111735 PMID: 34020251

12.   Huang L, Lyu Q, Zheng W, Yang Q, Cao G. Traditional application and modern pharmacological research of Eucommia ulmoides Oliv. Chin Med. 2021; 16:73. https://doi.org/10.1186/s13020-021-00482-7 PMID: 34362420

13.   Sih CJ, Ravikumar PR, Huang FC, Buckner C, Whitlock H Jr. Letter: Isolation and synthesis of pinoresinol diglucoside, a major antihypertensive principle of Tu-Chung(Eucommia ulmoides, Oliver). J Am Chem Soc. 1976; 98:5412–3. https://doi.org/10.1021/ja00433a070 PMID: 956566

14.   Yan D, Si W, Zhou X, Yang M, Chen Y, Chang Y, et al. Eucommia ulmoides bark extract reduces blood pressure and inflammation by regulating the gut microbiota and enriching the Parabacteroides strain in high-salt diet and N(omega)-nitro-L-arginine methyl ester induced mice. Front Microbiol. 2022; 13:967649. https://doi.org/10.3389/fmicb.2022.967649 PMID: 36060766

15.   Jiang L, Wang Z, Zhu HW, Di HY, Li H, Zhang YY, et al. Beneficial effect of Eucommia polysaccharides on systemic lupus erythematosus-like syndrome induced by Campylobacter jejuni in BALB/c mice. Inflammation. 2011; 34:402–11. https://doi.org/10.1007/s10753-010-9247-7 PMID: 20814813

16.   Ye R, Guo Q, Huang J, Wang Z, Chen Y, Dong Y. Eucommia ulmoides polysaccharide modified nano-selenium effectively alleviated DSS-induced colitis through enhancing intestinal mucosal barrier function and antioxidant capacity. J Nanobiotechnology. 2023; 21:222. https://doi.org/10.1186/s12951-023-01965-5 PMID: 37438752

17.   Chen Y, Pan R, Zhang J, Liang T, Guo J, Sun T, et al. Pinoresinol diglucoside (PDG) attenuates cardiac hypertrophy via AKT/mTOR/NF-κB signaling in pressure overload-induced rats. J Ethnopharmacol. 2021; 272:113920. https://doi.org/10.1016/j.jep.2021.113920 PMID: 33607200

18.   Wu QQ, Xiao Y, Duan MX, Yuan Y, Jiang XH, Yang Z, et al. Aucubin protects against pressure overload-induced cardiac remodelling via the β(3)-adrenoceptor-neuronal NOS cascades. Br J Pharmacol. 2018; 175:1548–66. https://doi.org/10.1111/bph.14164 PMID: 29447430

19.   Hung TC, Zhao N, Huang C, Liu S, Liu T, Huang W, et al. Exploring the mechanism of PingTang No.5 capsule on nonalcoholic fatty liver disease through network pharmacology and experimental validation. Biomed Pharmacother. 2021; 138:111408. https://doi.org/10.1016/j.biopha.2021.111408 PMID: 33684693

20.   Zhang W, Chen Y, Jiang H, Yang J, Wang Q, Du Y, et al. Integrated strategy for accurately screening biomarkers based on metabolomics coupled with network pharmacology. Talanta. 2020; 211:120710. https://doi.org/10.1016/j.talanta.2020.120710 PMID: 32070601

21. Benet LZ, Hosey CM, Ursu O, Oprea TI. BDDCS, the Rule of 5 and drugability. Adv Drug Deliv Rev. 2016; 101:89–98. https://doi.org/10.1016/j.addr.2016.05.007 PMID: 27182629

22. He H, Liu P, Li P. Dexmedetomidine Ameliorates Cardiac Ischemia/Reperfusion Injury by Enhancing Autophagy Through Activation of the AMPK/SIRT3 Pathway. Drug Des Devel Ther. 2023; 17:3205–18. https://doi.org/10.2147/DDDT.S428024 PMID: 37908314

23. Wang Z, Yang N, Hou Y, Li Y, Yin C, Yang E, et al. L-Arginine-Loaded Gold Nanocages Ameliorate Myocardial Ischemia/Reperfusion Injury by Promoting Nitric Oxide Production and Maintaining Mitochondrial Function. Adv Sci (Weinh). 2023; 10:e2302123. https://doi.org/10.1002/advs.202302123 PMID: 37449329

24. Xiang M, Liu T, Tian C, Ma K, Gou J, Huang R, et al. Kinsenoside attenuates liver fibro-inflammation by suppressing dendritic cells via the PI3K-AKT-FoxO1 pathway. Pharmacol Res. 2022; 177:106092. https://doi.org/10.1016/j.phrs.2022.106092 PMID: 35066108

25. Chen L, Liu Y, Wang Z, Zhang L, Xu Y, Li Y, et al. Mesenchymal stem cell-derived extracellular vesicles protect against abdominal aortic aneurysm formation by inhibiting NET-induced ferroptosis. Exp Mol Med. 2023; 55:939–51. https://doi.org/10.1038/s12276-023-00986-2 PMID: 37121969

26. Lin F, Yang Y, Wei S, Huang X, Peng Z, Ke X, et al. Hydrogen Sulfide Protects Against High Glucose-Induced Human Umbilical Vein Endothelial Cell Injury Through Activating PI3K/Akt/eNOS Pathway. Drug Des Devel Ther. 2020; 14:621–33. https://doi.org/10.2147/DDDT.S242521 PMID: 32103904

27. Xue R, Lei S, Xia ZY, Wu Y, Meng Q, Zhan L, et al. Selective inhibition of PTEN preserves ischaemic post-conditioning cardioprotection in STZ-induced Type 1 diabetic rats: role of the PI3K/Akt and JAK2/STAT3 pathways. Clin Sci (Lond). 2016; 130:377–92. https://doi.org/10.1042/CS20150496 PMID: 26666444

28. He F, Xu BL, Chen C, Jia HJ, Wu JX, Wang XC, et al. Methylophiopogonanone A suppresses ischemia/reperfusion-induced myocardial apoptosis in mice via activating PI3K/Akt/eNOS signaling pathway. Acta Pharmacol Sin. 2016; 37:763–71. https://doi.org/10.1038/aps.2016.14 PMID: 27063216

29. Tepebaşı MY, Aşcı H, Özmen Ö, Taner R, Temel EN, Garlı S. Cannabidiol ameliorates lipopolysaccharide-induced cardiovascular toxicity by its antioxidant and anti-inflammatory activity via regulating IL-6, Hif1α, STAT3, eNOS pathway. Mol Biol Rep. 2024; 51:825. https://doi.org/10.1007/s11033-024-09772-3 PMID: 39023749

30. Ozcan MS, Savran M, Kumbul Doguc D, Kubra Dogan H, Altintas M, Cosan S. Dexpanthenol ameliorates lipopolysaccharide-induced cardiovascular toxicity by regulating the IL-6/HIF1α/VEGF pathway. Heliyon. 2024; 10:e24007. https://doi.org/10.1016/j.heliyon.2024.e24007 PMID: 38268590

31. Heidari Z, Naeimzadeh Y, Fallahi J, Savardashtaki A, Razban V, Khajeh S. The Role of Tissue Factor In Signaling Pathways of Pathological Conditions and Angiogenesis. Curr Mol Med. 2024; 24:1135–51. https://doi.org/10.2174/0115665240258746230919165935 PMID: 37817529

32. López B, Ravassa S, San José G, Latasa I, Losada-Fuentenebro B, Tapia L, et al. Circulating biomarkers of myocardial remodelling: current developments and clinical applications. Heart. 2024: https://doi.org/10.1136/heartjnl-2024-323865 PMID: 39117384

33. Huang HM, Jiang X, Hao ML, Shan MJ, Qiu Y, Hu GF, et al. Identification of biomarkers in macrophages of atherosclerosis by microarray analysis. Lipids Health Dis. 2019; 18:107. https://doi.org/10.1186/s12944-019-1056-x PMID: 31043156

34. Ushio-Fukai M, Alexander RW. Reactive oxygen species as mediators of angiogenesis signaling: role of NAD(P)H oxidase. Mol Cell Biochem. 2004; 264:85–97. https://doi.org/10.1023/b:mcbi.0000044378.09409.b5 PMID: 15544038

35. Lesnefsky EJ, Hoppel CL. Ischemia-reperfusion injury in the aged heart: role of mitochondria. Arch Biochem Biophys. 2003; 420:287–97. https://doi.org/10.1016/j.abb.2003.09.046 PMID: 14654068

36. Shan S, Liu Z, Guo T, Wang M, Tian S, Zhang Y, et al. Growth arrest-specific gene 6 transfer promotes mesenchymal stem cell survival and cardiac repair under hypoxia and ischemia via enhanced autocrine signaling and paracrine action. Arch Biochem Biophys. 2018; 660:108–20. https://doi.org/10.1016/j.abb.2018.10.016 PMID: 30365934

37. Mattay SS, Zamani M, Saturno D, Loftus EV Jr, Ciorba MA, Yarur A, et al. Risk of Major Adverse Cardiovascular Events in Immune-Mediated Inflammatory Disorders on Biologics and Small Molecules: Network Meta-Analysis. Clin Gastroenterol Hepatol. 2024; 22:961–70.e12. https://doi.org/10.1016/j.cgh.2023.09.033 PMID: 37821035

38. Bauersachs J, König T, van der Meer P, Petrie MC, Hilfiker-Kleiner D, Mbakwem A, et al. Pathophysiology, diagnosis and management of peripartum cardiomyopathy: a position statement from the Heart Failure Association of the European Society of Cardiology Study Group on peripartum cardiomyopathy. Eur J Heart Fail. 2019; 21:827–43. https://doi.org/10.1002/ejhf.1493 PMID: 31243866

39. Shah MS, Brownlee M. Molecular and Cellular Mechanisms of Cardiovascular Disorders in Diabetes. Circ Res. 2016; 118:1808–29. https://doi.org/10.1161/CIRCRESAHA.116.306923 PMID: 27230643

40. Song P, Yakufujiang Y, Zhou J, Gu S, Wang W, Huo Z. Identification of important genes related to anoikis in acute myocardial infarction. J Cell Mol Med. 2024; 28:e18264. https://doi.org/10.1111/jcmm.18264 PMID: 38526027

41. Zhang Q, Wang L, Wang S, Cheng H, Xu L, Pei G, et al. Signaling pathways and targeted therapy for myocardial infarction. Signal Transduct Target Ther. 2022; 7:78. https://doi.org/10.1038/s41392-022-00925-z PMID: 35273164

42. Huang J, Chen L, Wu J, Ai D, Zhang JQ, Chen TG, et al. Targeting the PI3K/AKT/mTOR Signaling Pathway in the Treatment of Human Diseases: Current Status, Trends, and Solutions. J Med Chem. 2022; 65:16033–61. https://doi.org/10.1021/acs.jmedchem.2c01070 PMID: 36503229

43. Semenza GL. Hypoxia-inducible factors: roles in cardiovascular disease progression, prevention, and treatment. Cardiovasc Res. 2023; 119:371–80. https://doi.org/10.1093/cvr/cvac089 PMID: 35687650

44. Tarhriz V, Abkhooie L, Moradi Sarabi M. Regulation of HIF-1 by MicroRNAs in Various Cardiovascular Diseases. Curr Cardiol Rev. 2023; 19:51–6. https://doi.org/10.2174/1573403X19666230330105259 PMID: 37005512

45. Baldini C, Moriconi FR, Galimberti S, Libby P, De Caterina R. The JAK-STAT pathway: an emerging target for cardiovascular disease in rheumatoid arthritis and myeloproliferative neoplasms. Eur Heart J. 2021; 42:4389–400. https://doi.org/10.1093/eurheartj/ehab447 PMID: 34343257

46. Zhang J, Jiang H, Liu DH, Wang GN. Effects of dexmedetomidine on myocardial ischemia-reperfusion injury through PI3K-Akt-mTOR signaling pathway. Eur Rev Med Pharmacol Sci. 2019; 23:6736–43. https://doi.org/10.26355/eurrev_201908_18565 PMID: 31378917

47. Wang Y, Guan X, Gao CL, Ruan W, Zhao S, Kai G, et al. Medioresinol as a novel PGC-1α activator prevents pyroptosis of endothelial cells in ischemic stroke through PPARα-GOT1 axis. Pharmacol Res. 2021; 169:105640. https://doi.org/10.1016/j.phrs.2021.105640 PMID: 33915296

48. Hwang JH, Hwang IS, Liu QH, Woo ER, Lee DG. (+)-Medioresinol leads to intracellular ROS accumulation and mitochondria-mediated apoptotic cell death in Candida albicans. Biochimie. 2012; 94:1784–93. https://doi.org/10.1016/j.biochi.2012.04.010 PMID: 22534194

49. Jang WY, Kim MY, Cho JY. Antioxidant, Anti-Inflammatory, Anti-Menopausal, and Anti-Cancer Effects of Lignans and Their Metabolites. Int J Mol Sci. 2022; 23:15482. https://doi.org/10.3390/ijms232415482 PMID: 36555124